PERGAMON

Corrosion Science 43 (2001) 1657–1674

CORROSION SCIENCE

www.elsevier.com/locate/corsci

Localized alkaline corrosion of alloy AA5083 in neutral 3.5% NaCl solution

A. Aballe [a], M. Bethencourt [a], F.J. Botana [a,*], M.J. Cano [a], M. Marcos [b]

[a] *Departamento de Ciencia de los Materiales e Ingeniería Metalúrgica y Química Inorgánica, Facultad de Ciencias del Mar, Universidad de Cádiz, Polígono Río San Pedro s/n. Apdo. 40, Puerto Real, 11510-Cádiz, Spain*

[b] *Departamento de Ingeniería Mecánica y Diseño Industrial, Escuela Superior de Ingeniería, Universidad de Cádiz. c/Sacramento, 82, 11003-Cádiz, Spain*

Received 17 February 2000; accepted 9 October 2000

Abstract

The corrosion process of the alloy AA5083 in an aerated solution of NaCl at 3.5% has been studied. The results obtained indicate that the main process that this alloy undergoes, under the conditions of exposure studied, is related to localized corrosion that takes place as a consequence of the process of alkalinization around the cathodic precipitates existing in the alloy. The pitting formed presents a hemispherical morphology that is clearly different from crystallographic pitting. The formation of crystallographic pitting has not been observed, even in samples submitted to tests of very long duration. In order to obtain the formation of crystallographic pitting, it is necessary to polarize the alloy at the nucleation potential of pitting and, in addition, the density of the current must be above a critical value. Only when the layer of oxide is eliminated does the formation of crystallographic pitting take place by simple exposure in an aerated solution of NaCl at 3.5%.

Keywords: Aluminum alloy; Intermetallics; SEM; Pitting corrosion

* Corresponding author. Tel.: +34-956-016154; fax: +34-956-016040.
E-mail address: javier.botana@uca.es (F.J. Botana).

0010-938X/01/$ - see front matter
PII: S0010-938X(00)00166-9

1. Introduction

Corrosion by pitting in aluminum alloys is a complex process that can be affected by diverse experimental factors such as the pH, the temperature, the type of anion present in the solution or the physico-chemical characteristics of the passive layer [1]. The adsorption of aggressive ions such as Cl^- into the faults in the protective film, and their penetration and accumulation in these imperfections is considered one of the triggering factors of the process of nucleation of pitting [2–4]. Other authors have suggested that pits may develop as a result of a process of hydrolysis which gives rise to a local reduction of the pH which, in turn, impedes the subsequent process of repassivation [5].

Equally, another factor which is associated with the susceptibility of aluminum to pitting corrosion and other forms of localized corrosion is the electrochemical nature of the intermetallic phases [6–8]. Thus, often its corrosion behavior is correlated with the difference in potential between the matrix and the intermetallic compounds present in the alloy [9–13]. In Ref. [8], it is proposed that the presence of metallic inclusions more noble than the matrix reduces the resistance of the alloy to corrosion. By acting as cathodes, these inclusions provoke a process of anodic dissolution in the surrounding matrix [14,15]. The first research work on this proposition involved the study of the effect of the presence of Al_3Fe inclusions on the corrosion behavior of the alloys in which these inclusions are present [16,17]. According to the findings of these studies, the presence of Al_3Fe precipitates increases the susceptibility of the alloy to pitting corrosion. The local increase in pH which is produced as a consequence of the reduction reaction of O_2 is indicated as a possible cause of the formation of pits around the intermetallic compounds. In Ref. [18] the researchers managed to determine a local increase in pH in the metal surrounding the Al_3Fe inclusions.

The pits produced by the presence of intermetallic cathodes have been designated as alkaline pits in Ref. [15]. This type of pitting is formed below the potentials of nucleation and repassivation. From the information available in the literature, it is not clear whether any relationship exists between this type of attack and the pitting known as crystallographic which is formed when alloys reach the pitting nucleation potential. On this point, in the review of aluminum corrosion by pitting published in this same journal [15], reference is made to the need for more in-depth studies of this type of phenomenon.

In the present paper, the processes of corrosion of the alloy AA5083 (Al–Mg) in aerated solutions of NaCl at 3.5% are studied. The research has been directed towards studying the characteristics, conditions of formation and morphology of attack which takes place at open circuit potential.

2. Experimental

The materials studied are samples of the aluminum–magnesium alloy AA5083, the composition of which, as determined by ICP, is given in Table 1.

Table 1
Composition of the alloy AA5083 (% by mass)

Mg	Mn	Si	Fe	Ti	Cu	Cr	Al
4.9	0.5	0.13	0.3	0.03	0.08	0.13	Rest

The samples used to conduct the various tests were pieces of the alloy AA5083 $20 \times 20 \times 5$ mm^3, wet-sanded mechanically with SiC papers of 220 and 500 grits. Before use, samples were de-greased with ethanol of 99% purity and then rinsed with plenty of distilled water.

In the cases where it was necessary, the corrosion products were eliminated by immersion of the samples in HNO_3 at 70% for 2 min and then washed with plenty of distilled water.

As the aggressive medium, an aerated solution of NaCl at 3.5% and at pH 5.5 was used. This solution was prepared dissolving 3.5 ± 0.1 parts by weight of NaCl in 96.5 ± 0.1 parts of distilled water.

The immersion tests were conducted at 303 K in a cell constructed in accordance with ASTM Standard G-31 [19]. Two cells were used in each test with a total of 12 samples, which remained in the solution for periods ranging from 1 to 30 days.

The SEM studies were conducted with a JEOL 820-SM scanning microscope equipped with a LINK AN-10000 dispersive energy analyzer. The optical microscope studies were conducted with a Nikon Optiphot metallographic microscope equipped with a CCD camera (Sony model Iris) connected to a PC.

The electrochemical measurements were made in a Parc EG&G K235 flat cell, coupled to a Solartron model 1287 potentiostat. A Crison model 52–40 Ag/AgCl electrode was used as the reference electrode; the potential of this electrode with respect to NHE is −0.207 V.

3. Results and discussion

3.1. Microstructural characterization of the alloy AA5083

In order to identify the various types of intermetallic compounds present in the alloy AA5083, samples polished to mirror quality were studied using the optical microscope, the SEM and EDS spectroscopy.

Using the scanning microscope, three different types of intermetallic compounds were identified; the composition of these was then determined by EDS spectroscopy (Fig. 1). The results obtained indicate that particles such as those shown in Fig. 1(a) mostly consist of Al, Mn, Fe, and Cr; those shown in Fig. 1(b) basically contain Al, Si and Mg; while those shown in Fig. 1(c) mainly contain Al and Mg. The composition of these intermetallics matches that observed by various other authors for the same alloy [20,21].

It is significant that, in addition to the differences in composition, there exist notable differences in the particle size of each of the intermetallic compounds

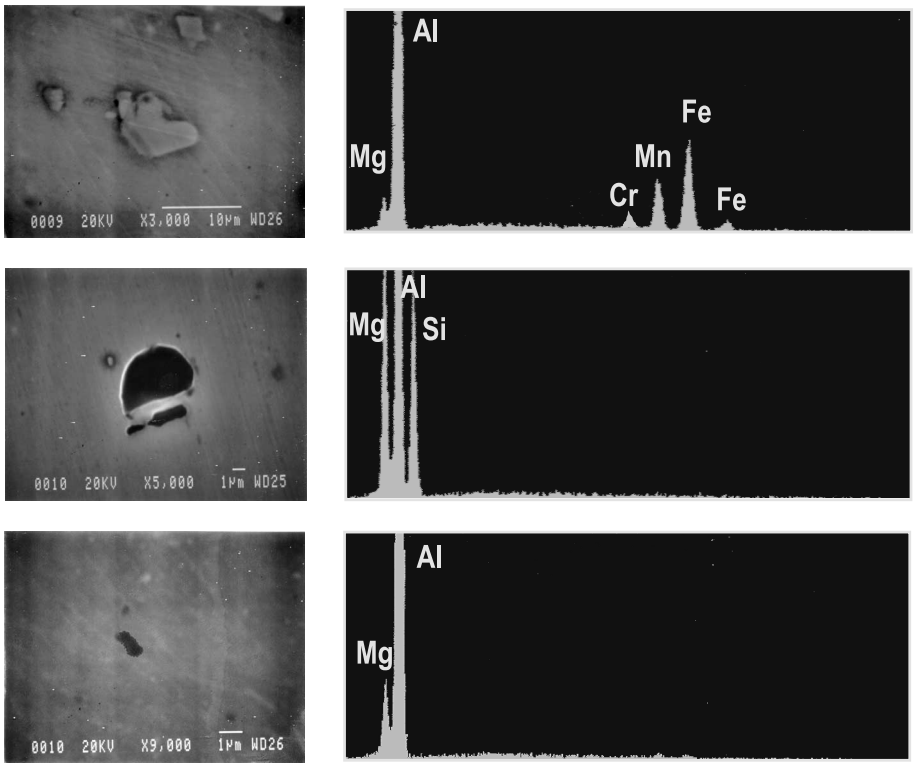

Fig. 1. SEM images of the different intermetallics identified in samples of alloy AA5083, polished to mirror quality. EDS spectra recorded on (a) Al(Mn,Fe,Cr); (b) Al(Si,Mg); (c) Al–Mg.

identified. With regard to the Al(Mn,Fe,Cr) precipitates, it was confirmed that there exist two maxima in the distribution of particle sizes: one type of particle was found with a mean size of about 100 μm^2 while the surface area of the other type is approximately 1 μm^2. The particles of Al(Si,Mg) presented an area of approximately 30 μm^2 and those of Al–Mg approximately 6 μm^2.

Similarly, there existed differences in respect of the number of particles of each type present on the surface; the most abundant are those of Al(Mn,Fe,Cr) whereas those of Al–Mg are the least numerous [6].

Fig. 2(a) shows the image obtained with the metallographic microscope corresponding to a sample of alloy AA5083 polished to mirror quality. In this type of image, the precipitates of Al(Mn,Fe,Cr) are those that appear in the dark tone (point 1) while those of Al(Si,Mg) appear in a lighter tone (point 2). With the optical microscope it is difficult to identify precipitates of Al–Mg due to their small size and their color being similar to that of the matrix. To make them visible it is necessary to provoke metallographic attacks; thus in Fig. 2(b) these precipitates can be seen in a sample subjected to an attack with HNO_3 for 10 s.

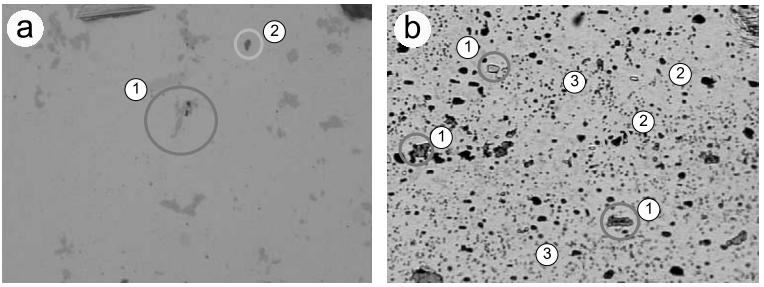

Fig. 2. Optical microscope images, 200×, (a) sample polished to mirror quality; (b) treated for 10 s in HNO_3 at 10%; intermetallics identified (1) Al(Mn,Fe,Cr); (2) Al(Si,Mg); (3) Al–Mg.

3.2. SEM/EDS study of the behavior of samples of alloy AA5083 in solutions of NaCl at 3.5%

In this section are presented the results obtained from the SEM/EDS study of the behavior of samples of the alloy AA5083 subjected to total immersion tests in aerated solutions of NaCl at 3.5%. The duration of the tests varied from 1 to 30 days. The samples subjected to these tests were studied first before removing the products of the corrosion process and then after their removal in a solution of HNO_3 at 70%.

Fig. 3(a) shows the SEM image of a sample after a test of 1 day's duration. Although the period of exposure is relatively short, the existence of a localized attack

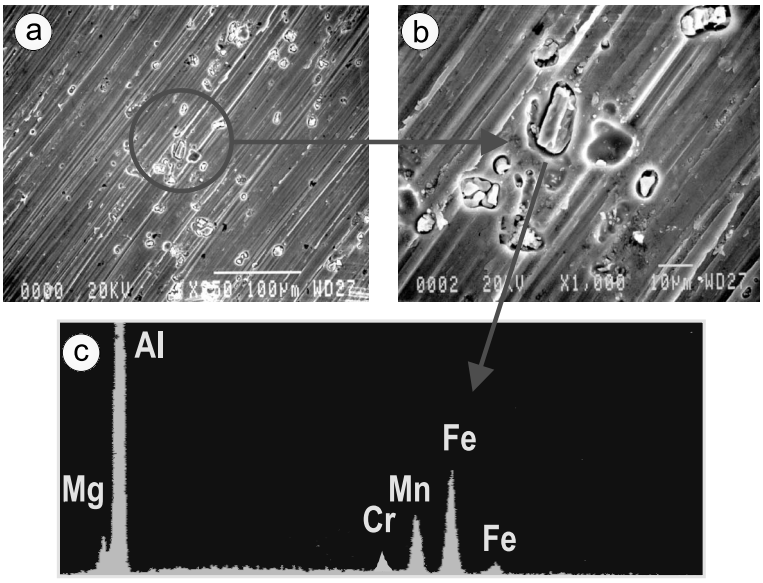

Fig. 3. (a) SEM image obtained from a sample of alloy AA5083 after 24 h of exposure in an aerated solution of NaCl at 3.5%; (b) SEM image of one of the Al(Mn,Fe,Cr) precipitates; (c) EDS spectrum acquired on the precipitate (b).

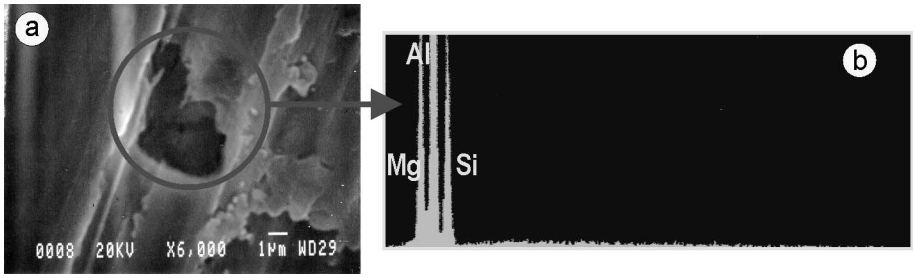

Fig. 4. (a) SEM image of an Al(Si,Mg) intermetallic in a sample of alloy AA5083 after 24 h of immersion in an aerated solution of NaCl at 3.5%; (b) EDS spectrum obtained on this intermetallic.

on various points of the surface of the sample can be observed. Fig. 3(b) shows an image at greater magnification in which it can be seen that, for this time of exposure, the attack is localized to the zones adjacent to particular precipitates in the matrix.

The dispersive energy spectra recorded for these particles (Fig. 3(c)) confirm that the attack is localized to zones where there are precipitates of Al(Mn,Fe,Cr). A second characteristic of these samples is the formation of cavities (Fig. 3(b)), the origin of which is discussed later in this paper. It is significant that for this length of exposure no attack is observed on the body of the matrix nor in those zones where other types of precipitate are present (Fig. 4).

This latter finding can be more clearly appreciated in the images obtained using the metallographic microscope. In Fig. 5(a), it is shown an image corresponding to a sample newly polished to mirror-quality; Fig. 5(b) is an image of the same sample after an immersion test of 72 h. Both images are of exactly the same zone so that a comparison between them allows the evolution of each type of precipitate to be monitored. Comparing the precipitates of Al(Mn,Fe,Cr), marked as 1, in both figures, it can be observed that the process of corrosion provokes a notable change in these zones; in contrast, the precipitates of Al(Si,Mg), marked 2, remain practically unchanged.

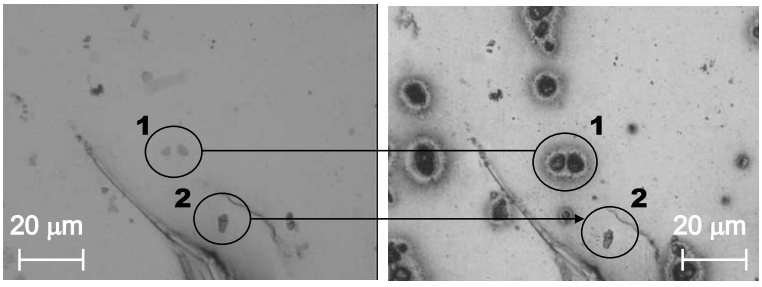

Fig. 5. Image taken with a metallographic microscope for a sample of alloy AA5083 before and after 72 h of immersion in an aerated solution of NaCl at 3.5%. Point 1: Al(Mn,Fe,Cr) precipitate; point 2: Al(Si,Mg) precipitate.

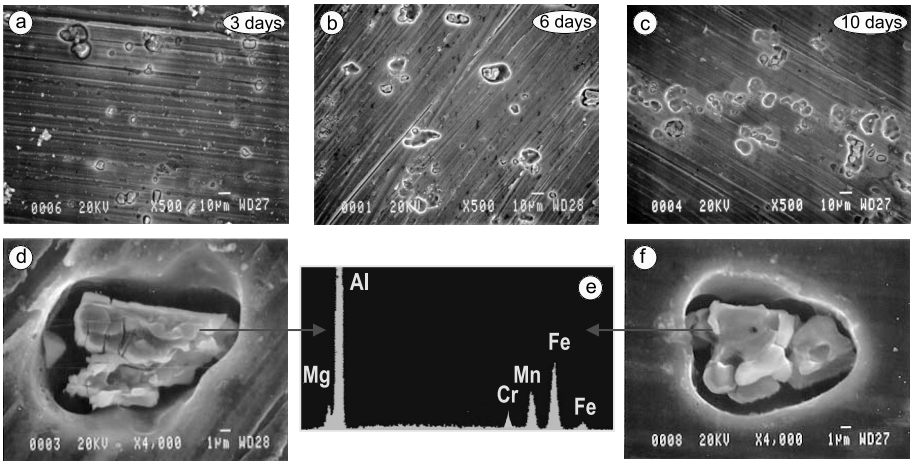

Fig. 6. SEM images of samples treated by immersion in an aerated solution of NaCl at 3.5% for the periods of time indicated: (a) 3 days; (b) 6 days; (c) 10 days; (d–f) detail and EDS spectrum of Al(Mn, Fe,Cr) precipitates.

The pattern of behavior presented by the samples after the first day of exposure does not undergo much modification during the rest of the first 10 days. Fig. 6(a)–(e) show the SEM micrographs recorded for exposure times of 3, 6 and 10 days. In these it can be observed that the same type of attack is present. As the time of immersion increases, slight changes can be seen in the topography of the samples, with an increase in the number of cavities (Fig. 6(c)).

After 12 days of exposure, certain zones of the surface of the sample acquire a distinct contrast to the rest of the surface (Fig. 7(a)). These differences disappear on treating the samples with a solution of HNO_3 at 70%. This suggests that these contrasts are due to the development of a surface layer of corrosion products. The EDS spectra recorded for these zones (Fig. 7(b)) show practically no difference from

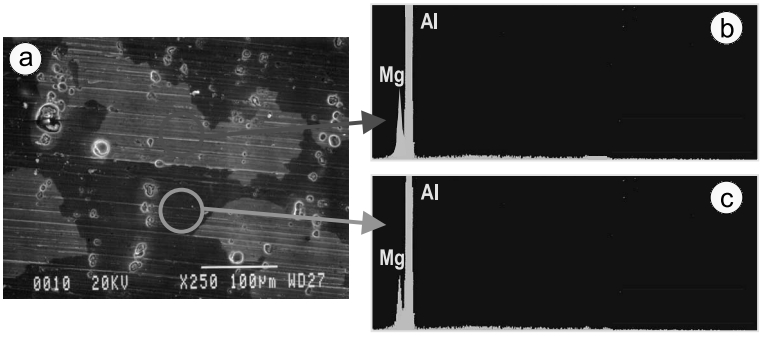

Fig. 7. (a) SEM image of the surface contrasts seen on a sample of alloy AA5083 after 12 days of immersion in an aerated solution of NaCl at 3.5%; (b and c) EDS spectra obtained on each of the zones.

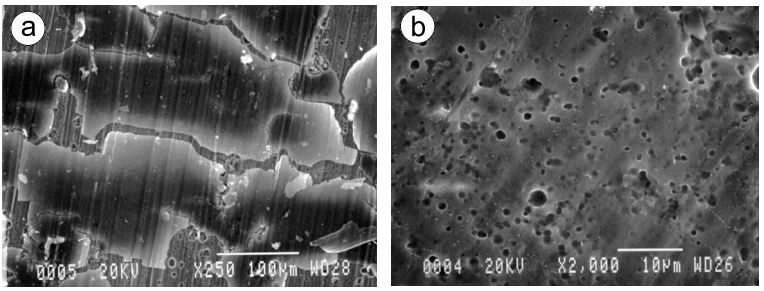

Fig. 8. (a) SEM image of a sample of alloy AA5083 after 15 days of immersion in an aerated solution of NaCl at 3.5%; (b) descaled sample: detail of the micropits observed after 15 days of immersion.

those recorded for the matrix. The proportion of the surface occupied by this layer increases with the exposure time.

From 15 days of immersion, notable changes in the samples begin to be produced. Firstly, as it can be observed in a sample that has not been descaled, Fig. 8(a), the surface film has grown in thickness and extends to cover most of the surface area. The fracturing of this layer may be the consequence of its drying. Secondly, once the sample has been descaled, it is observed that there are a large number of small hemispherical pits of approximately 1 μm diameter, that had not been detected on samples exposed for shorter periods of time (Fig. 8(b)).

In the samples subjected to tests for periods of duration from 15 to 30 days, the only significant modification observed is the increase in the thickness of the layer, there being no change in the morphology of the attack (Fig. 9).

It can be concluded from the results obtained using SEM/EDS that, under the conditions of exposure studied, the alloy AA5083 in a 3.5% solution of NaCl suffers a process of localized corrosion. This process affects the zones of the matrix in contact with the Al(Mn,Fe,Cr) intermetallics. This phenomenon appears from the first day of exposure.

From the tenth day of exposure, a film of oxide is observed to develop over the surface of the sample; this increases in area and in thickness with the passage of time.

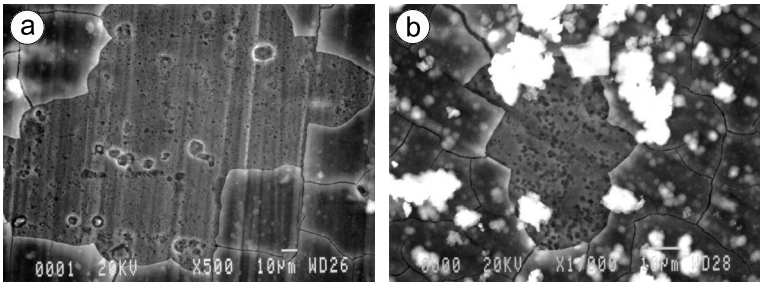

Fig. 9. SEM images of a sample of alloy AA5083 after (a) 25 days and (b) 30 days of immersion in an aerated solution of NaCl at 3.5%.

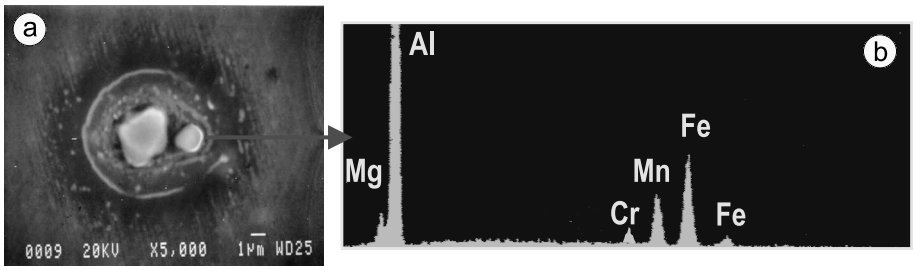

Fig. 10. (a) SEM image of an Al(Mn,Fe,Cr) precipitate after a galvanostatic treatment at -50 μA/cm^2 for 15 min; (b) EDS spectrum obtained on this precipitate.

The development of this film does not prevent the formation of cavities and large numbers of hemispherical micropits during prolonged exposures; these extend over a high proportion of the total area.

In order to study this phenomenon in greater depth for purposes of interpretation of the SEM data obtained, galvanostatic experiments were conducted subjecting the system to both anodic and cathodic polarization. Firstly, galvanostatic treatment was applied polarizing the samples cathodically at a current density of -50 μA/cm^2 for 15 min. Similarly, anodic polarizations were conducted galvanostatically, working at current densities of 50 μA/cm^2 for 15 min.

Fig. 10(a) shows the SEM image corresponding to a sample subjected to cathodic polarization treatment. Here it can be observed how the action of this treatment translates into a localized attack around the precipitates of Al(Mn,Fe,Cr) (Fig. 10(b)).

Attacks with a similar morphology have been described by various authors when subjecting aluminum alloys to cathodic polarization treatment [22] or in basic media [14]. In the case we are dealing with, even though neutral solutions are being used, these precipitates present a cathodic behavior with respect to the matrix [21]. For this reason, there will be a preferential reaction of oxygen reduction on this type of precipitate.

In Ref. [23], Davenport et al. detected local increases of pH in the cathodic places in alloy AA2024 which are associated with processes of oxygen reduction. Similarly, Park et al. [18] made measurements of the variations in pH in the area surrounding the AlFe intermetallics of alloy AA6061, using a selective microelectrode. These authors found a strong increase in pH in the pits formed around the inclusions.

In summary, in agreement with the information reported in the bibliography, the cathodic character of the Al(Mn,Fe,Cr) precipitates causes the reaction of oxygen reduction to be produced on them [23]. This reaction would produce a local increase of the pH, causing the layer of oxide around the precipitate to dissolve. Once the layer of oxide has been dissolved, the local alkalinization produces an intense attack in the matrix–precipitate interface which finally gives rise to the formation of hemispherical pits (Fig. 8).

The relationship between the formation of the hemispherical pits and the processes of local alkalinization in the surroundings of the cathodic precipitates is

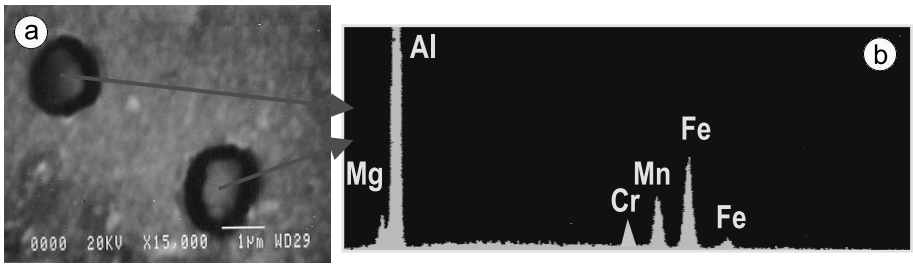

Fig. 11. (a) SEM image of an Al(Mn,Fe,Cr) precipitate of 1 μm diameter after a galvanostatic treatment at −50 μA/cm^2 for 15 min; (b) EDS spectrum obtained on this precipitate.

supported by the fact that this type of attack is similar in appearance to that observed by other authors in basic media [14]. Secondly, the intensity of the process is accentuates when the samples are cathodically polarized (Fig. 10(a)). In these conditions, the cathodic process occurs more intensely and, therefore, the effect of the local increase in pH is sharper, thus intensifying the corrosion of the matrix in the zone surrounding the Al(Mn,Fe,Cr) precipitates (Fig. 10(a)). After these treatments, the existence of small precipitates of Al(Mn,Fe,Cr) of approximately 1 μm diameter is observed (Fig. 11); in the area around these, the same type of attack as that described for precipitates of the same kind but of larger size can be appreciated.

In Fig. 10(a) it can also be observed that, after these tests of cathodic polarization, the zones of the samples in the proximity of which there are no Al(Mn,Fe,Cr) precipitates present are not evidently affected. Further, in those zones where other kinds of precipitates are present, such as Al(Si,Mg) for example, no type of alteration can be seen (Fig. 12).

The morphology of the attack produced in the samples when they are polarized anodically is considerably different from that produced by cathodic polarization. As can be observed in Fig. 13, the treatment of the samples at 50 μA/cm^2 for 15 min

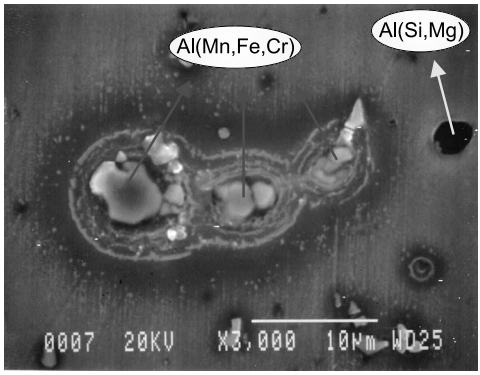

Fig. 12. SEM image of a set of Al(Mn,Fe,Cr) and Al(Si,Mg) precipitates after a galvanostatic treatment at −50 μA/cm^2 for 15 min.

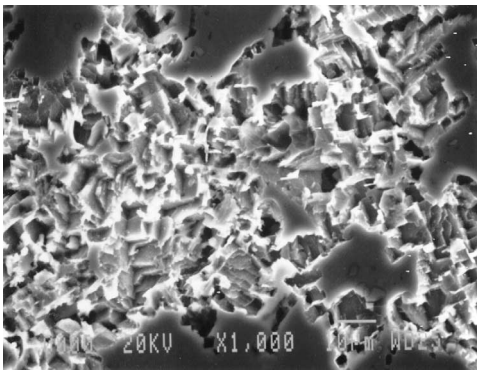

Fig. 13. SEM image of a crystallographic pit after a galvanostatic treatment at 50 μA/cm^2 for 15 min.

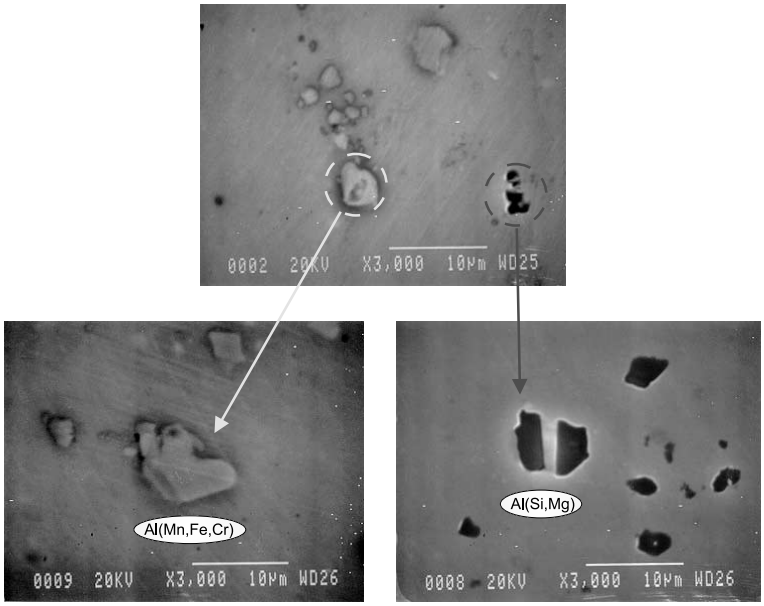

Fig. 14. SEM image of a set of Al(Mn,Fe,Cr) and Al(Si,Mg) precipitates after a galvanostatic treatment at 50 μA/cm^2 for 15 min.

leads to the formation of crystallographic pitting, similar to that described in Ref. [22] for alloy AA5086 or in Ref. [24] for pure aluminum. It should be noted that the two types of precipitate that are mainly present in the alloy, Al(Mn,Fe,Cr) and Al(Si,Mg), are not found to be affected by this type of treatment. It can be deduced, therefore, that there does not appear to exist any relationship between the formation of crystallographic pitting and the existence of intermetallic particles (Fig. 14).

If the results obtained from the galvanostatic tests are compared with those from the study at open circuit potential, two basic conclusions may be drawn. First, those crystallographic pits are not formed on the exposure of the samples of alloy AA5083 in aerated solutions of NaCl at 3.5%. Second, the morphology of the attack observed in samples subjected to immersion tests coincides to a large extent with that observed in the cathodically polarized samples (Figs. 3 and 10(a)). It can thus be assumed that in these samples the local increase in pH produced on the cathodic precipitates has the effect of causing the layer of oxide in surrounding areas to dissolve and the exposed matrix then to be attacked.

The appearance of the alkaline pitting could be produced by the complete solution of the cathodic precipitates as a consequence of the alkalinization of the medium [14] or by a simple detachment by action of gravity when the area of contact between the matrix and the intermetallic particle is reduced (Fig. 15). Data included in Ref. [25] would support this second hypothesis, since a strong dependence has been observed between the disposition of the sample during exposure (horizontal or vertical) and the appearance of the hemispherical pits. But whatever their mechanism of formation, the cavities observed in the micrographs corresponding to the samples treated at open circuit potential (Fig. 6) are associated with the disappearance of the cathodic precipitates. The small pits observed after longer periods of treatment could have their origin in a similar mechanism acting on precipitates of the same kind but of smaller size (Fig. 8).

The findings discussed here so far demonstrate that the exposure of alloy AA5083 at open circuit potential leads to its localized corrosion but not to the appearance of crystallographic pitting. In principle, these data should cause surprise, bearing in mind that the potential of corrosion of the sample, -0.760 V, is close to that of the pitting nucleation, -0.720 V [26].

With the object of discovering the explanation for this kind of behavior, samples were polarized anodically at various current densities ranging from 0.1 to 50 $\mu A/cm^2$ for 15 min. In Fig. 16 are presented the SEM images corresponding to samples treated at current densities above 0.5 $\mu A/cm^2$. It may be noticed, firstly, that the type of pitting produced is that known as crystallographic. Secondly, it is observed that, as the density of the current applied increases, the number and size of these pits also increase. The crystallographic nature of the pits produced can be observed in greater detail in Fig. 17. Furthermore, the intermetallic compounds and the areas surrounding them are not affected in the treatments that lead to the formation of crystallographic pits (Fig. 18).

In contrast, when the current applied is less than 0.1 $\mu A/cm^2$, the formation of this type of pitting is not observed, for treatment times of 15 min (Fig. 16). It was necessary to increase the current to 0.5 $\mu A/cm^2$ in order to detect the existence of small crystallographic pitting.

At the lowest of the current densities applied in these tests, 0.1 $\mu A/cm^2$, the duration of the test was extended to 24 h, but even so, no crystallographic pitting was observed. Under these conditions, the type of attack observed in the cathodic polarization treatments is reproduced (Fig. 19). This phenomenon may be due to the fact that, when polarizing at relatively low anodic currents, the residual cathodic

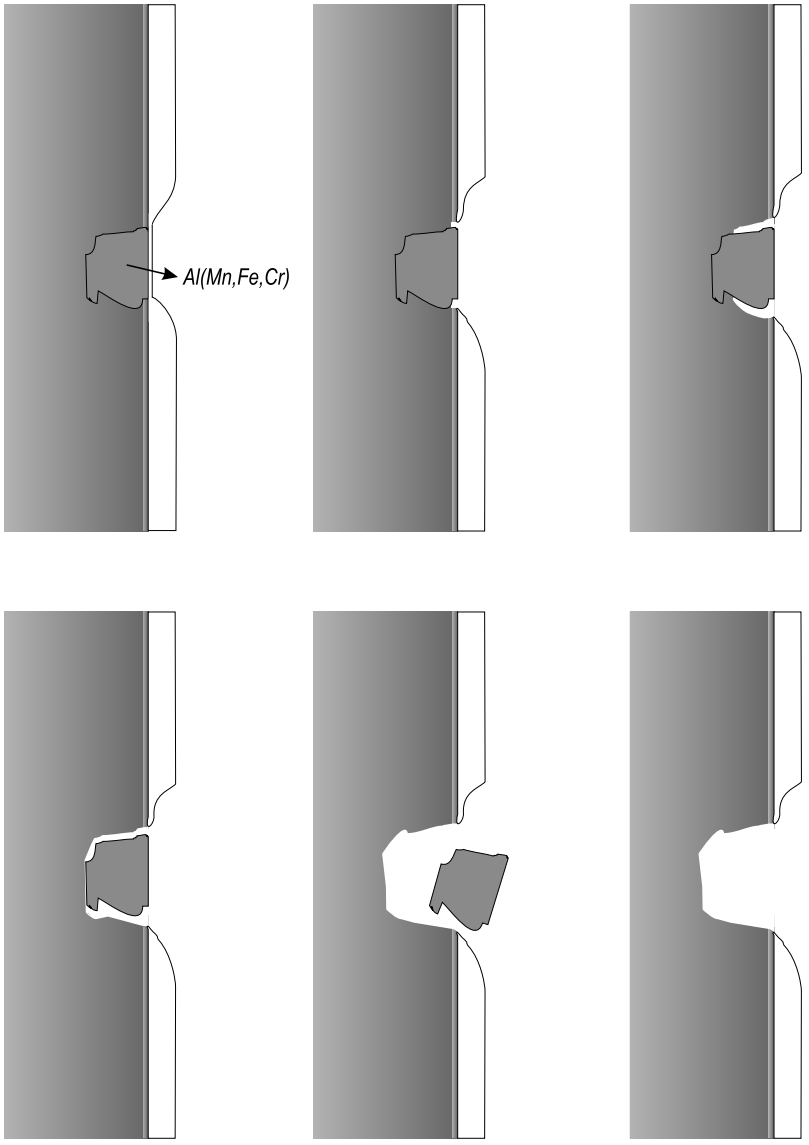

Fig. 15. Model of the process of formation of cavities by localized alkaline corrosion.

current is still high enough to provoke local increases in pH, which may explain the appearance of this type of attack.

To develop crystallographic pitting without having to activate anodically the sample, it was necessary to carry out a prior potentiostatic treatment at –840 mV in the 3.5% NaCl solution for 1 h. At the end of this period, the sample was left to reach the open circuit potential, which in this case was −720 mV. Once this potential was

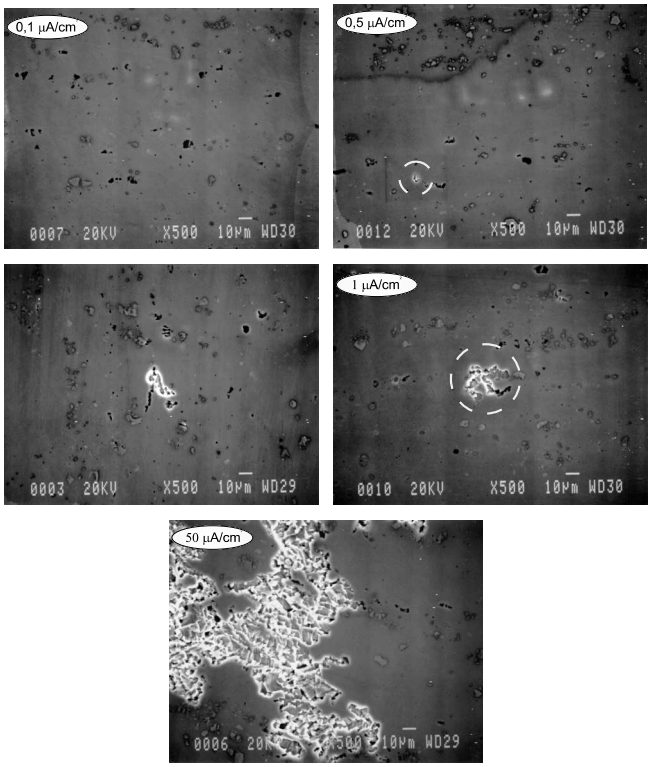

Fig. 16. SEM images of samples of alloy AA5083 after galvanostatic tests at 0.1–50 μA/cm^2 for 15 min in solutions of NaCl at 3.5%.

stable, the system was maintained under these conditions for 1 h. Fig. 20 shows the SEM image of the sample obtained after this treatment, in which it can be confirmed that, effectively, there co-exist zones presenting localized alkaline corrosion formed during the polarization at −840 mV, and other zones presenting crystallographic pitting generated at −720 mV. In this sample, the cathodic polarization, as well as producing the localized corrosion around the Al(Mn,Fe,Cr) precipitates, must have caused the dissolution of the oxide film formed during its manipulation. When this film is removed, the value of the open circuit potential changes to the nucleation potential of pitting of the matrix, with the resulting formation of crystallographic pitting.

If this treatment is carried out on a sample previously treated in a solution of NaCl, only alkaline corrosion is observed. In this case, the open circuit potential that is reached after the cathodic polarization is −760 mV. The interpretation of these findings is that the polarization treatment is not sufficient to dissolve the layer formed by immersion. The existence of this layer prevents the formation of crystallographic pitting.

Finally, the existence of chlorides in the medium does not appear to be a sufficient condition for alkaline pitting to take place. The results reported in Ref. [27] show

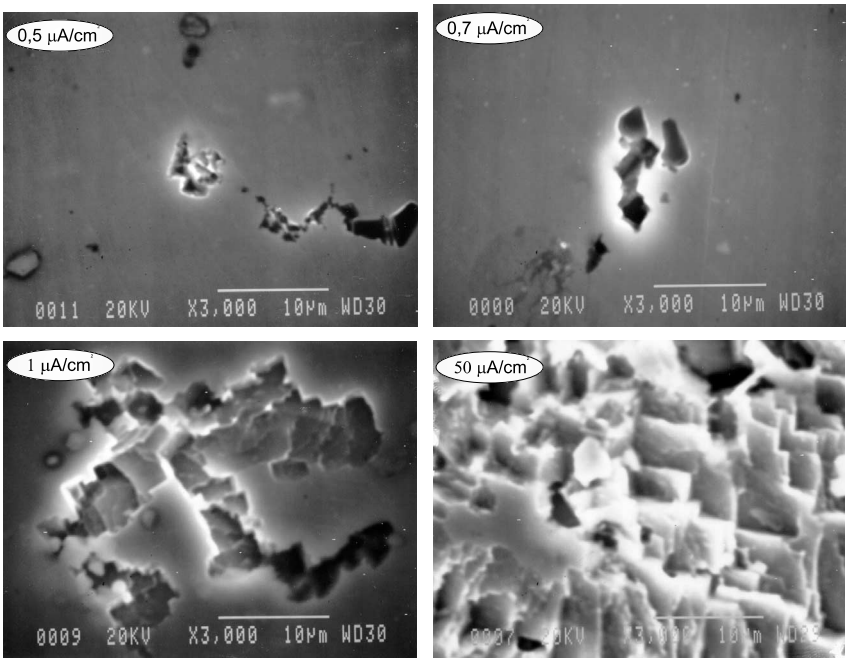

Fig. 17. SEM images of samples of alloy AA5083 after galvanostatic tests at 0.1–50 μA/cm^2 for 15 min in solutions of NaCl at 3.5%: details of crystallographic pitting.

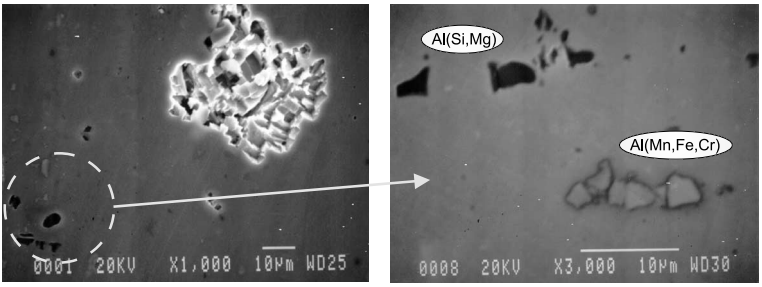

Fig. 18. SEM image of a sample of alloy AA5083 after a galvanostatic test at 1 μA/cm^2 for 15 min in a solution of NaCl at 3.5%: details of crystallographic pitting and of the Al(Mn,Fe,Cr) and Al(Si,Mg) intermetallics.

that when working with inhibiting solutions, such as $CeCl_3$ for example, and with a concentration of NaCl in the medium of 3.5%, the formation of alkaline pits is not observed with exposure periods of up to 30 days. In accordance with these results, the addition of $CeCl_3$ has a blocking effect on the cathodic zones that prevents an increase in pH from occurring; such an increase would occur in solutions without the inhibitor [27]. These results demonstrate that when the cathodic activity in the

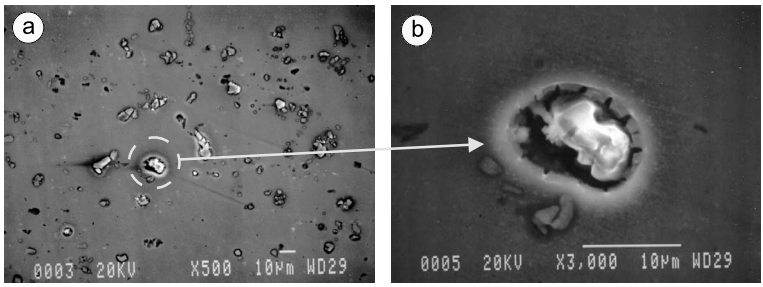

Fig. 19. (a) SEM image of a sample of alloy AA5083 after a galvanostatic test at 0.1 μA/cm^2 for 24 h in a solution of NaCl at 3.5%; (b) detail of alkaline corrosion surrounding an intermetallic of Al(Mn,Fe,Cr).

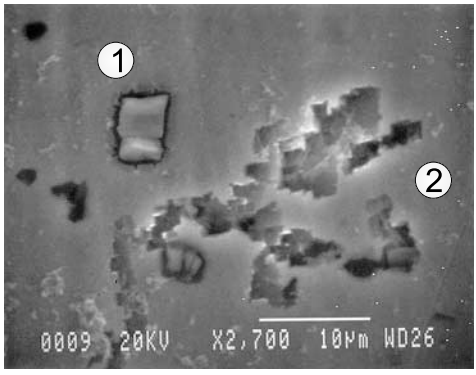

Fig. 20. SEM image of a sample of subjected to a potentiostatic test at −840 mV for 1 h and then at open circuit for 1 h. Coexistence of localized alkaline corrosion (1) and crystallographic pitting (2).

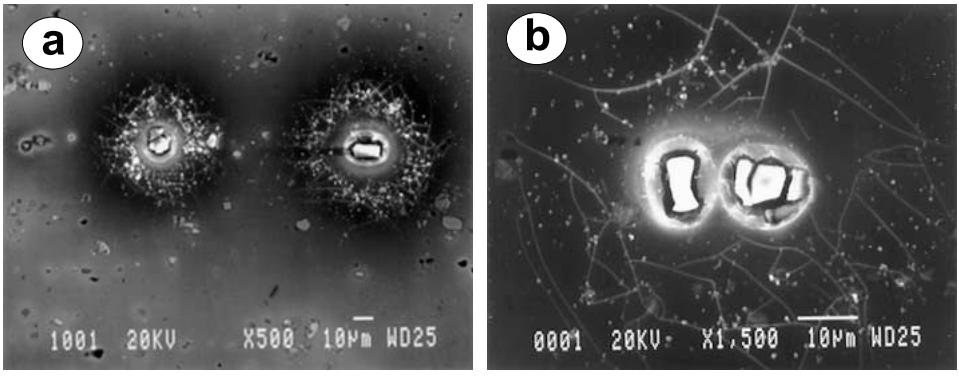

Fig. 21. (a) SEM image of a sample of alloy AA5083 after two days of immersion in distilled water; (b) detail of alkaline corrosion surrounding an intermetallic of Al(Mn,Fe,Cr).

system is low, alkaline pitting is not produced even with a high level of chlorides present in the medium.

In addition, if immersion tests are conducted in distilled water, alkaline pits are observed from the first hours of exposure (Fig. 21). These results would indicate that, while the presence of chlorides may accelerate the process, it is not an essential prerequisite for processes of localized alkaline corrosion to take place. It would be necessary to take additional measurements to obtain more conclusive results regarding the role of chlorides in this type of phenomenon.

4. Conclusions

From this study of the corrosion behavior of alloy AA5083 in a 3.5% NaCl solution, it can be concluded that, in function of the conditions of treatment, this alloy undergoes two types of localized corrosion process, leading to the formation of hemispherical and crystallographic pits.

In agreement with the results obtained when alloy AA5083 corrodes freely in a solution of NaCl at 3.5%, the samples undergo a process of corrosion localized to the area surrounding the precipitates of Al(Mn,Fe,Cr), which results in hemispherical pits. Under these conditions of exposure, no evidence has been found of the formation of crystallographic pitting, even for exposure times up to 30 days.

The data obtained demonstrate that this type of corrosion is related to the cathodic activity of these precipitates. The local increase in pH that is produced as a consequence of the reduction reaction would give rise to the local dissolution of the layer of oxide and to the subsequent dissolution of matrix in contact with the precipitate. The cavities observed in the samples are the result of the disappearance of the precipitates of Al(Mn,Fe,Cr), possibly by simple detachment.

For the formation of crystallographic pitting to be produced, it is necessary to polarize the alloy at the nucleation potential of pitting or to apply a constant anodic current at a density above a critical level. Only in the case when the layer of oxide has been destroyed does the formation of this type of pitting take place by the simple exposure of the alloy in an aerated solution of NaCl at 3.5%.

Acknowledgements

This work has received financial support from Comision Interministerial de Ciencia y Tecnología (CICYT), projects MAT99-0625-C02-01 and 1FD97-0333-C03-02, and the Junta de Andalucía.

References

[1] Z. Szklarska-Smialowska, Pitting Corrosion of Metals, NACE, Houston, 1986, p. 3.
[2] H.H. Strehblow, Mechanism of pitting corrosion, in: P. Marcus, J. Oudart (Eds.), Corrosion Mechanism in Theory and Practice, Marcel Dekker, New York, 1995.

[3] J.B. Bessone, D.R. Salinas, C.E. Mayer, M. Ebert, W.J. Lorenz, Electrochim. Acta 37 (1992) 2283.
[4] A.G. Muñoz, J.B. Bessone, Corr. Sci. 41 (7) (1999) 1447.
[5] J.R. Galvele, J. Electrochem. Soc. 123 (1976) 464.
[6] M. Bethencourt, F.J. Botana, J.J. Calvino, M. Marcos, J. Pérez, M.A. Rodríguez, Mater. Sci. Forum 289–292 (1998) 567.
[7] A. Alavi, R. Cottis, Corros. Sci. 27 (1987) 443.
[8] K. Nisancioglu, J. Electrochem. Soc. 137 (1) (1990) 69.
[9] H. Vosskühler, H. Zeiger, Aluminum 37 (1961) 424.
[10] W.W. Binger, E.H. Hollingsworth, D.O. Sprowls, in: K.R. Van Horn (Ed.), Aluminum, vol. 1: Properties Physical Metallurgy and Phase Diagrams, ASM, Ohio, 1967.
[11] K. Goto, Y. Shimizu, G. Ito, Trans. Nat. Res. Inst. Met. 22 (1980) 86.
[12] M. Zamin, Corrosion 37 (1981) 627.
[13] O. Seri, N. Matsuko, J. Electrochem. Soc. 32 (1982) 303.
[14] E.V. Koroleva, G.E. Thompson, G. Hollrigl, M. Bloeck, Corros. Sci. 41 (8) (1999) 1475.
[15] Z. Szklarska-Smialowska, Corros. Sci. 41 (9) (1999) 1743.
[16] G.A.W. Murray, H.J. Lamb, H.P. Godard, Br. Corros. J. 2 (1967) 216.
[17] P.M. Aziz, H.P. Godard, Corrosion 10 (9) (1954) 269.
[18] J.O. Park, C.H. Paik, R.C. Alkire, in: P.M. Natishan, R.G. Kelly, G.S. Frankel, R.C. Newman (Eds.), Critical Factors in Localized Corrosion II, The Electrochem. Soc, Pennington, NJ, 1996.
[19] ASTM Recommended Practice for Laboratory Inmersion Corrosion Testing of Metals, G-31, Annual Book of ASTM Standards, ASTM, Philadelphia, 1994.
[20] L.F. Mondolfo, Aluminum Alloys: Structure and Properties, Butterworths, 1976.
[21] G.A. Gehring, M.H. Peterson, Corrosion 37 (4) (1981) 232.
[22] Ph. Giménez, J.J. Rameau, M.C. Rebioul, Corrosion 37 (12) (1981) 673.
[23] A.J. Aldykewicz, H.S. Isaac, A.J. Davenport, J. Electrochem. Soc. 143 (1) (1996) 147.
[24] G.C. Wood, H.W. Sutton, J.A. Richardson, T.N.K. Riley, A.G. Malherbe, Localized Corrosion, International Corrosion Conference Series NACE-3, 1986, p. 526.
[25] M. Bethencourt, Ph.D. Thesis, University of Cádiz, 1999.
[26] J.R. Galvele, S.M. de Micheli, I.L. Muller, S.B. de Wexler, I.L. Alanis, in: R. Staehle, B. Brown, J. Kruger, A. Agrawal (Eds.), Critical Potentials for Localized Corrosion of Aluminum Alloys, vol NACE-3, National Asociation of Corrosion Engineers, Houston, 1974.
[27] M. Bethencourt, F.J. Botana, M. Marcos, M.A. Arenas, J.J. de Damborenea, Corros. Sci. 43 (1) (2001) 157.